Carcinogenesis vol.26 no.2 pp.309–318, 2005
doi:10.1093/carcin/bgh329

Peptides specific to the galectin-3 carbohydrate recognition domain inhibit metastasis-associated cancer cell adhesion

Jun Zou[1], Vladislav V.Glinsky[1,2], Linda A.Landon[2], Leslie Matthews[3] and Susan L.Deutscher[1,2,*]

[1]Department of Biochemistry, University of Missouri, Columbia, MO 65212, USA, [2]Harry S.Truman Memorial Veteran's Hospital, Columbia, MO 65201, USA and [3]Dana-Farber Cancer Institute, Boston, MA 02115, USA

*To whom correspondence should be addressed at: Department of Biochemistry, M743 Medical Sciences Building, Columbia, MO 65212, USA. Tel: +1 573 882 2454; Fax: +1 573 884 4597; Email: deutschers@missouri.edu

Intravascular cancer cell adhesion plays a significant role in the metastatic process. Studies indicate that galectin-3, a member of the galectin family of soluble animal lectins, is involved in carbohydrate-mediated metastatic cell heterotypic (between carcinoma cells and endothelium) and homotypic (between carcinoma cells) adhesion via interactions with the tumor-specific Thomsen–Friedenreich glycoantigen (TFAg). We hypothesized that blocking the galectin-3 carbohydrate recognition domain with synthetic peptides would significantly reduce metastasis-associated carcinoma cell adhesion. To test this hypothesis, we identified peptide antagonists of the galectin-3 carbohydrate recognition domain using combinatorial bacteriophage display technology. The peptides bound with high affinity to purified recombinant galectin-3 protein ($K_d \approx$ 17–80 nM) and to cell surface galectin-3. Experiments with a series of recombinant serially truncated galectin-3 mutants indicated that the peptides bound the carbohydrate recognition domain of galectin-3. Furthermore, the peptides did not bind the carbohydrate recognition domain of other galectins and plant lectins. Synthetic galectin-3 carbohydrate recognition domain-specific peptides blocked the interaction between galectin-3 and TFAg and significantly inhibited rolling and stable heterotypic adhesion of human MDA-MB-435 breast carcinoma cells to endothelial cells under flow conditions, as well as homotypic tumor cell aggregation. These results demonstrate that carbohydrate-mediated, metastasis-associated tumor cell adhesion could be inhibited efficiently with short synthetic peptides which do not mimic naturally occurring glycoepitopes yet bind to the galectin-3 carbohydrate recognition domain with high affinity and specificity.

Introduction

Metastasis is a complex process consisting of multiple steps. Metastasis-associated events initiate with release of cancer cells from a primary lesion, migration into the bloodstream (1) and binding to the endothelium in target organ microvessels (2). Two forms of metastasis-related tumor cell adhesion, heterotypic adhesion between neoplastic and endothelial cells and homotypic adhesion of tumor cells to each other, are involved in metastasis (3). Both heterotypic and homotypic cancer cell adhesion are mediated in part by specific interactions between cell surface lectins and their cognate carbohydrate ligands presented on glycoproteins and glycolipids (3–7).

Galectin-3 is the predominant member of the galectin family of soluble mammalian lectins recognizing terminal β-galactopyranose. Galectin-3 may facilitate metastasis by promoting tumor cell adhesion (7,8) and invasiveness (9), as well as by antagonizing tumor cell apoptosis (10–12) and inducing endothelial cell proliferation and angiogenesis (13). Galectin-3 is prominently expressed in several types of cancer (14,15) and its expression correlates with tumor cell transformation and metastatic phenotype *in vivo* (16). Elevated galectin-3 expression significantly enhances tumor cell adhesion to common extracellular matrix proteins (17), increases the incidence of lung metastases (16) and protects cancer cells from apoptosis (10–12). Furthermore, pretreatment of tumor cells with an anti-galectin-3 antibody reduces the incidence of metastatic lung colonies by up to 90% (18). These data suggest that galectin-3 expression and interactions with its cognate carbohydrate ligands could be important in tumor metastasis.

We previously demonstrated that the cancer-associated Thomsen–Friedenreich glycoantigen (TFAg), a galactose β1-3 *N*-acetylgalactosamine disaccharide (19) exposed on up to 90% of human carcinomas (19,20), is one of the major galectin-3 carbohydrate ligands present on cancer cells (21). Increased levels of TFAg correlate with metastasis in gastric (22), colorectal (23) and breast carcinomas (24). Recent works suggest that galectin-3 expressed on endothelial cells may interact with carbohydrate ligands such as TFAg on carcinoma cells to mediate tumor cell adhesion and metastasis (21,25). Upon appropriate stimulation, endothelial galectin-3 is rapidly redistributed to the sites of tumor cell–endothelial cell contacts (3), suggesting that galectin-3–TFAg interactions might be important early steps in the formation of intravascular metastatic deposits. Inhibiting these steps could potentially modify metastasis-associated tumor cell adhesion and help in controlling metastatic cancer spread. Traditionally, such inhibition could be achieved using carbohydrate-based compounds interacting with the galectin-3 carbohydrate recognition domain (26,27). In this study we have tested the hypothesis that metastasis-associated heterotypic and homotypic adhesion of carcinoma cells mediated by interactions between galectin-3 and TFAg could be efficiently inhibited by small synthetic peptides which specifically and selectively bind to the galectin-3 carbohydrate recognition domain. Short synthetic peptides which bind to galectin-3 carbohydrate recognition domain with high affinity and specificity may represent yet another attractive alternative approach to inhibiting galectin-3 function and β-galactoside-mediated metastasis-associated tumor cell adhesion. Carbohydrate–lectin interactions usually occur in the mid-micromolar range (28–30). In contrast,

Abbreviations: ASF, asialofetuin; TFAg, Thomsen–Friedenreich glycoantigen.

peptide–protein interactions frequently occur with much higher affinity, in the nanomolar range (31,32). However, our laboratory has identified high affinity (K_d ~ 100 nM) carbohydrate-binding peptides (33,34). Thus, identifying peptides with high affinity that could block the corresponding carbohydrate recognition domains of carbohydrate-binding proteins may represent a valuable new approach to inhibiting functionally relevant carbohydrate–lectin interactions.

In this report, peptide antagonists of galectin-3 which bound to purified recombinant galectin-3 with high affinity were identified. The selected peptides specifically bound to the C-terminal carbohydrate recognition domain of galectin-3, but not to other lectins tested, and efficiently blocked the interaction of human recombinant galectin-3 with β-galactosides. Further, the galectin-3 carbohydrate recognition domain-specific peptides exhibited specific binding to galectin-3 expressed on tumor cells and inhibited homotypic adhesion of MDA-MB-435 human breast cancer cells as well as their heterotypic adhesion to endothelial cells under physiological flow conditions. These results demonstrate that β-galactoside-mediated, metastasis-associated tumor cell adhesion could be efficiently disrupted by small synthetic peptides that interact with the galectin-3 carbohydrate recognition domain with high affinity and specificity.

Materials and methods

Materials

All chemicals and reagents, unless specifically noted, were purchased from Sigma-Aldrich Chemical Co. (St Louis, MO).

Purification of recombinant galectin-3 and galectin-3 mutants

Full-length recombinant human galectin-3 was expressed in *Escherichia coli* from the vector pET3 (a generous gift from Dr Avraham Raz, Wayne State University, Detroit, MI). Recombinant human galectin-3 was purified using a β-lactose affinity chromatography matrix as previously described (35).

Four truncated proteins with N-terminal deletions were produced by cloning the full-length human galectin-3 cDNA into the vector pET15b (Novagen, Madison, WI). Mutants *Del*1-28 and *Del*1-63 were constructed by sequentially digesting galectin-3 plasmid DNA (*Del*1-28, NdeI and BstXI; *Del*1-63, NdeI and XcmI). The desired fragments were gel purified and recircularized using T4 DNA ligase. Mutants *Del*1-12 and *Del*1-118 were constructed using primer-directed mutagenesis. A common downstream primer (5′-GGGTACCGA GCTCGAATTC-3′) containing an EcoRI site was used. Distinct upstream primers introduced a unique BamHI restriction site (*Del*1-12, 5′-CGGG-ATCCGGGGTCTGGAAACCCAAACC-3′; *Del*1-118, 5′-CGGGATCCGAA CCTGCCTTTGCCTGGG-3′). The PCR products were gel purified, digested with appropriate restriction enzymes and ligated into the vector pET15b. All constructs were chemically transformed into the non-expression host strain JM109. Plasmid DNA was isolated and the mutations were confirmed by DNA sequencing (University of Missouri DNA Core Facility). The mutants were expressed in *E.coli* BL21 and purified using Ni-NTA columns (Qiagen, Valencia, CA).

The identity, purity and molecular weight of the recombinant proteins were analyzed using SDS–PAGE and immunoblotting with either monoclonal antibody TIB-116 (American Type Culture Collection), which binds an N-terminal epitope and recognizes the full-length and *Del*1-12, and *Del*1-28 galectin-3 proteins, or rabbit anti-galectin-3 polyclonal antibody (Dr Avraham Raz), which recognizes all proteins (13). Protein concentration was determined using a Micro BCA Protein Assay Reagent Kit (Pierce, Rockford, IL).

Affinity selection

Two random phage display libraries, f88/15 and f88/Cys6 (Dr George Smith, University of Missouri-Columbia) (36), each consisting of ~1×10^{11} phage clones encoding random 15 and 6 amino acid peptides, respectively, were used for affinity selection against purified recombinant galectin-3 as previously described (37). Briefly, galectin-3 was biotinylated using an Immunopure Sulfo-NHS-Biotin Kit (Pierce, Rockford, IL) according to the manufacturer's directions. Next, 4 μg biotinylated galectin-3 in 0.5% v/v Tween 20 in Tris-buffered saline was immobilized on streptavidin-coated dishes. Recombinant phage (10^{12} transforming units/ml) were added for 4 h at room temperature. The dishes were extensively washed. Bound phage particles were eluted with 0.22 M glycine–HCl, pH 2.2, and neutralized with Tris–HCl, pH 9.1. After each round of selection, phage were amplified for further use. After four rounds of selection, 80 individual phage clones were randomly picked and propagated independently. Redundant phage clones were eliminated using one-lane dideoxy DNA sequencing with a single termination mix (38). The coding sequences of the unique clones were determined using a modified dideoxy sequencing method as described previously (39).

Phage membrane binding assay

Phage membrane binding assays were conducted as described previously (34). Individual phage clones (2×10^8 virions) were spotted onto a nitrocellulose membrane and blocked. The membrane was incubated with 2 mg biotinylated galectin-3. Bound galectin-3 was detected colorimetrically using a streptavidin–horseradish peroxidase conjugate.

Peptide synthesis and purification

Peptides were chemically synthesized using solid phase Fmoc chemistry on an Advanced ChemTech 396 multiple peptide synthesizer (Advanced ChemTech, Louisville, KY) and purified by high pressure liquid chromatography. Biotin was covalently linked to the N-terminus of the peptide on the resin using a standard coupling agent for formation of the amide bond. All masses were verified by mass spectroscopy analysis.

Peptide binding and immunoblot analysis

Purified full-length and truncated galectin-3 proteins were separated by 12% SDS–PAGE (40) and transferred to nitrocellulose membranes, which were subsequently blocked with 6% bovine serum albumin for 1 h at room temperature and washed with Tween 20 in Tris-buffered saline. Next, the membranes were incubated with 20 μM solutions of either biotinylated anti-galectin-3 peptides (10 mM Tris, pH 7.5, 2% bovine serum albumin), anti-galectin-3 monoclonal antibody (1/200 dilution) or anti-galectin-3 polyclonal antibody (1/500 dilution) in Tween 20 in Tris-buffered saline for 1 h at room temperature and washed extensively with Tween 20 in Tris-buffered saline. The membranes were then incubated with streptavidin–horseradish peroxidase conjugate for peptides or the corresponding horseradish peroxidase-conjugated secondary antibody (anti-rat for anti-galectin-3 monoclonal antibody or anti-rabbit for anti-galectin-3 polyclonal antibody; Santa Cruz Biotechnology, Santa Cruz, CA). After extensive washing, binding was detected colorimetrically using the 4CN membrane peroxidase substrate system (Kirkegaard & Perry Laboratories, Gaithersburg, MD).

To determine binding specificity of the peptides, blotting experiments were performed with galectin-3, galectin-1 and galectin-4 (R & D Systems, Minneapolis, MN), as well as with *Aleuria aurantia* lectin, *Vicia villosa* lectin (Vector Laboratories, Burlingame, CA) and *Arachis hypogaea* lectin. Equivalent amounts of each lectin were separated by SDS–PAGE, transferred onto nitrocellulose membranes and incubated with biotinylated peptides, as described previously. Peptide binding was detected using an alkaline phosphatase–streptavidin conjugate (Gibco BRL, Gaithersburg, MD) and BCIP/NBT as substrate (Fisher Scientific, Pittsburgh, PA). Lectin membrane binding assays were conducted in a manner similar to phage membrane binding assays, with lectins (0.1 μg/μl) being spotted onto nitrocellulose, blocked, incubated sequentially with biotinylated peptides and streptavidin–alkaline phosphatase and developed colorimetrically.

Fluorescence quenching

Galectin-3 was fluorescently labeled using an AlexaFluor 488 Protein Labeling Kit (Molecular Probes, Eugene, OR) according to the manufacturers' instructions. High throughput fluorescence quenching analysis of peptide binding affinity was performed as described previously (41). AlexaFluor 488–galectin-3 (1 nM) was used as a fluorophore. Serial peptide dilutions were used as quenchers. The quantum fluorescence output (in c.p.m.) was read on a Fusion Universal Microplate Analyzer (Packard Bioscience, Meriden, CT), using a 485 ± 20 nm excitation filter and a 520 ± 20 nm emission filter. The autofluorescence of empty wells was subtracted from each reading prior to analysis. Percent decrease from maximum [$\{1 - (Q_{obs}/Q_{max}\} \times 100\%$] was calculated. Binding affinity was calculated using the Langmuir binding equation, $Y = (B_{max} \times X)/(K_d + X)$ (42) and GraphPad Prism 3.0 software, where K_d is the dissociation affinity constant, B_{max} the maximal binding and X the total peptide molar concentration. All titrations were performed in triplicate.

Cell lines and culture

The human breast cancer cell lines BT549, which does not express detectable levels of galectin-3 (10), and BT549*trans*, transfected with the cDNA encoding galectin-3 (Dr Avraham Raz), were used as a model system for differential galectin-3 expression (10). The mouse monocyte/macrophage cell line J744A (American Type Culture Collection) (43), was used as a positive control.

The human breast carcinoma cell line MDA-MB-435 (National Cancer Institute) and human prostate carcinoma cell line PC-3M (Dr Avraham Raz), both of which express moderate levels of galectin-3 (43), were also used. Cells were grown to confluence in RPMI 1640 medium (Gibco BRL, Grand Island, NY) supplemented with L-glutamine, 10% fetal bovine serum, sodium pyruvate and non-essential amino acids. The human bone marrow endothelial cell line HBME-1 (25), kindly provided by Dr Kenneth J.Pienta (University of Michigan, Ann Arbor, MI), which has been used in our laboratory (3,44) as a model of tumor cell adhesion to the microvasculature in heterotypic adhesion assays, was cultured in DMEM medium supplemented with L-glutamine, 10% fetal bovine serum and sodium pyruvate.

Cell surface binding

Laser scanning confocal microscopy was conducted as described previously (33). For each cell suspension, 1×10^4 cells were dried on a microscope slide and blocked. The slides were incubated with biotinylated peptide solutions (20 μM in 10 mM Tris, pH 7.5, 1% bovine serum albumin) or rat anti-galectin-3 monoclonal antibody for 1 h at room temperature. Binding was detected using 10 μg/ml NeutrAvidin-Texas Red (Molecular Probes) for peptides and AlexaFluor 488-conjugated anti-rat secondary antibody (Molecular Probes) for anti-galectin-3 monoclonal antibody (incubation for 30 min at room temperature in the dark). Laser scanning confocal microscopy was performed on a Bio-Rad MRC 600 confocal microscope (University of Missouri Molecular Cytology Core Facility).

Asialofetuin (ASF) binding to galectin-3

Briefly, 10 μg/ml biotinylated galectin-3 in 0.5 % v/v Tween 20 in Tris-buffered saline was immobilized on streptavidin-coated dishes. ASF was fluorescently labeled using a Molecular Probes AlexaFluor 488 protein labeling kit as directed. The plates were blocked with 2% bovine serum albumin in Tween 20 in Tris-buffered saline and washed extensively. Biotinylated galectin-3 (0.5 μg) was immobilized on streptavidin-coated Microtest 96-well plates (BD Biosciences, NJ). The wells were then incubated with 0.5 μg AlexaFluor 488-labeled ASF for 1 h in the presence or absence of competitors (*N*-acetyl-lactosamine, *Arachis hypogaea* lectin or sucrose). ASF possesses three O-linked desialylated TFAg disaccharide moieties (45) and three branched asparagine-linked oligosaccharides containing a total of nine *N*-acetyl-lactosamine sequences (46,47). The binding of ASF to immobilized galectin-3 was detected using a Fusion Universal Microplate Analyzer (Packard Instrument Co., Meriden, CT) with 485 ± 20 nm excitation and 520 ± 20 nm emission filters. All the assays were performed in triplicate and data were analyzed using GraphPad Prism 3.0 software.

Inhibition enzyme-linked immunosorbent assay (ELISA)

ASF (0.5 μg) was preabsorbed to a 96-well plate for 2 h at room temperature and blocked. Galectin-3 (0.5 μg) in the presence or absence of increasing concentrations (1–50 μM) of anti-galectin-3 peptides or 'scrambled' anti-galectin-3 control peptides (G3-C9s, DKFPPTLHPQSINPG; G3-H12s, PTHVTCKYCPAGNRDP) were added and incubated for 1 h at room temperature. Bound galectin-3 was detected colorimetrically using a rat anti-galectin-3 primary monoclonal antibody and an alkaline phosphatase-conjugated goat anti-rat secondary antibody and developed with *p*-nitrophenyl phosphate. The absorbance at 405 nm was recorded. The assay was performed in triplicate. The data were normalized using the GraphPad Prism 3.0 software package. The absorbance obtained without peptide was set as 100% and the inhibition by peptides was calculated as a decrease in the absorbance at 405 nm compared with the control (no peptide).

Homotypic aggregation assay

The ability of the anti-galectin-3 peptides to inhibit homotypic aggregation of MDA-MB-435 breast carcinoma cells was determined as previously described (27). Briefly, 500 μl of a single cell suspension (5×10^5 cells) was mixed with 500 μl of serum-free medium in the presence of increasing concentrations (0–25 μM final concentration) of anti-galectin-3 peptides or control peptide and agitated for 1 h at 37°C. Next, three 25 μl aliquots from each sample were spotted onto a microscope slide, dried for 1 h at room temperature and fixed overnight in formaldehyde vapor. Immediately prior to microscopic evaluation, 25 μl of phosphate-buffered saline was placed on each spot to facilitate viewing. The total number of cells and the number of cells in aggregates were counted in four random fields in each spot. The percent of cells in aggregates [(number of cells in aggregates/total number of cells) × 100] and the average number of aggregated cells was calculated for individual samples. Each assay was performed in triplicate. The results, analyzed using GraphPad Prism 3.0 software, are presented as means ± SD.

Carcinoma cell adhesion to endothelial cell monolayer under flow conditions

The effects of anti-galectin-3 peptides on rolling and stable adhesion of MDA-MB-435 human breast carcinoma cells to endothelial cells under conditions of physiological shear stress were determined in an *in vitro* parallel plate laminar flow chamber as described previously (3). A human bone marrow endothelial cell line, HBME-1 (25), was used in parallel flow chamber experiments. HBME-1 cells were exposed to flow conditions (0.8 dyn/cm^2 shear stress) by perfusing warm medium (RPMI containing 0.75 mM Ca^{2+} and Mg^{2+} and 0.2 % human serum albumin) using a constant infusion/withdrawal syringe pump KDS210 (KD Scientific, New Hope, PA). Next, the flow chamber was perfused for 15 min with a MDA-MB-435 single cell suspension (1×10^4 cell/ml) in the presence or absence of 20 μM anti-galectin-3 peptides or control peptide. Tumor cell interactions with HBME-1 monolayers were observed using an inverted phase contrast Diavert microscope (Leitz, Wetzlat, Germany) and video recorded for subsequent frame-by-frame analysis. The percent of rolling cells and number of stably adherent cells per field was determined over 1 and 5 min time periods, respectively, in at least three different observation fields for each experimental setting. The data are presented as the means ± SD of three observation fields from one representative experiment.

Results

Isolation of galectin-3-binding peptides

Galectin-3-specific peptides were selected by screening both a random 15 amino acid and a cysteine-constrained library displayed on coat protein VIII. By the fourth round of selection, the output phage yield from both libraries was ~100-fold higher compared with the first round phage yield (data not shown), which indicated enrichment of galectin-3-binding phage clones in the eluted phage population. G3-A9 and G3-C12 were the predominant output clones (Table I).

In a phage membrane binding assay, six immobilized clones from the final round appeared to bind to galectin-3 (Figure 1A). Of these, G3-A9 and G3-C12 bound with the strongest intensities. Similar results were obtained from a phage capture-ELISA, which detected phage bound by immobilized galectin-3 (data not shown).

Binding affinity of synthesized peptides

Four peptides identified in the affinity selections were chemically synthesized. Three corresponded to the foreign sequences encoded by phage giving the strongest binding signals (G3-A9, G3-C9 and G3-C12) in the phage membrane binding assay and one corresponded to the predominant clone from the selection (G3-A3). G3-A9 represents the first 15 amino acids of a triple insert in the phage genome Fluorescence spectroscopy titration (41) was used to determine the

Table I. Results of combinatorial selections against galectin-3: deduced peptide sequences, percent occurrence of phage clones and affinity of peptides

Name	Peptide sequence	Library	Percent of clones[a]	Affinity (K_d) (nM)
G3-A3	SMEPALPDWWWKMFK	f88-15	8.8	17.7 ± 9.4 (K_d^1) 4.2 ± 2.3 (K_d^2)
G3-A4	DKPTAFVSVYLKTAL	f88-15	1.3	NA
G3-A9	PQNSKIPGPTFLDPH	f88-15	10.0	72.2 ± 32.8
G3-A18	APRPGPWLWSNADSV	f88-15	1.3	NA
G3-A19	GVTDSSTSNLDMPHW	f88-15	1.3	NA
G3-A28	PKMTLQRSNIRPSMP	f88-15	1.3	NA
G3-A29	PQNSKIPGPTFLDPH	f88-15	1.3	NA
G3-A40	LYPLHTYTPLSLPLF	f88-15	1.3	NA
G3-C4	LTGTCLQYQSRCGNTR	f88-Cys6	1.3	NA
G3-C9	AYTKCSRQWRTCMTTH	f88-Cys6	1.3	5.7 ± 2.2
G3-C12	ANTPCGPYTHDCPVKR	f88-Cys6	80.0	72.2 ± 32.8
G3-C44	NISRCTHPFMACGKQS	f88-Cys6	1.3	NA
G3-C60	PRNICSRRDPTCWTTY	f88-Cys6	1.3	NA

[a]The percentage of individual clones that were represented in the populations of 80 f88-15 and 60 f88-Cys6 libraries selected.

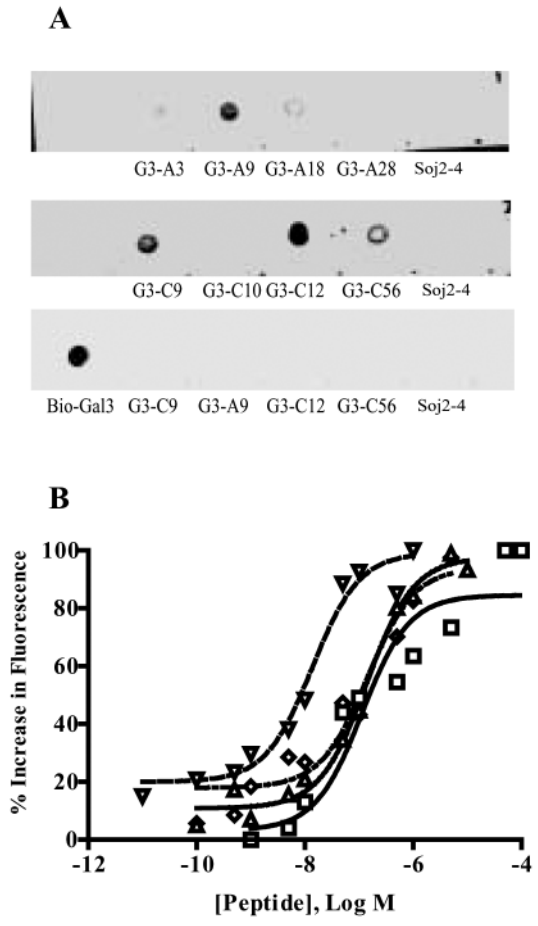

Fig. 1. Phage-displayed and chemically synthesized anti-galectin-3 peptides bind to galectin-3. (**A**) Peptides displayed on immobilized phage bind to galectin-3 in solution. Individual galectin-3 peptide phage clones (G3-A3, G3-A9, G3-A18 and G3-A28) or negative control phage (Soj24) were spotted onto a nitrocellulose membrane and incubated with biotinylated galectin-3 (in solution) and streptavidin–horseradish peroxidase conjugate (first two panels) or streptavidin–horseradish peroxidase conjugate only (third panel). (**B**) Dose-dependent quenching of AlexaFluor 488 fluorescence by galectin-3-binding peptides. Dose-dependent quenching of AlexaFluor 488 fluorescence by peptides was analyzed using the Langmuir binding equation and reported as $K_d \pm$ SEM. Error bars were eliminated for clarity. G3-A3 (squares) $K_d^1 = 17.9 \pm 9.4$ nM, $K_d^2 = 4.2 \pm 2.3$ μM; G3-A9 (diamonds) $K_d = 72.2 \pm 32.8$ nM; G3-C12 (triangles) $K_d = 88.0 \pm 23.0$ nM; G3-C9 (inverted triangles) $K_d = 5.7 \pm 2.2$ nM.

dissociation constant (K_d) describing the binding of peptides to galectin-3. Non-linear regression analysis of the dose-dependent increase in fluorescence (Figure 1B) indicated that G3-C9 had the highest affinity ($K_d = 5.7 \pm 2.2$ nM) for galectin-3, with maximal binding observed at 0.5 μM. Peptides G3-A9 ($K_d = 72.2 \pm 32.8$ nM) and G3-C12 ($K_d = 88.0 \pm 23.0$ nM) exhibited 10-fold lower affinities compared with G3-C9 (Table I). Maximal binding of G3-A9 and G3-C12 to galectin-3 was observed at concentrations between 1 and 10 μM. For all peptides except G3-A3, the range of 10–90% saturation fell within a 100-fold concentration range, indicating specific non-cooperative binding. Non-linear regression analysis of fluorescence quenching by peptide G3-A3 indicated that the binding isotherm best fitted a two-site binding algorithm ($K_d^1 = 17.9$ nM, $K_d^2 = 4.2$ μM). Thus, G3-A3 was eliminated from further study.

Peptide specificity

Galectin-3 possesses a single carbohydrate recognition domain located at the C-terminal end of the protein (48), which could be involved in tumor cell adhesion by interacting with cancer-associated cell surface carbohydrate ligands (21). Thus, we were interested in determining whether any of the selected peptides preferentially bound to the C-terminal carbohydrate recognition domain region of galectin-3. To define the region of galectin-3 recognized by the synthetic peptides, a series of truncated galectin-3 proteins with deletions of 12, 28, 63 and 118 amino acids from the N-terminus of the protein were generated (Figure 2A). Immunoblot analyses with anti-galectin-3 monoclonal antibody and polyclonal antibody permitted detection of full-length and truncated galectin-3 proteins (Figure 2B). The polyclonal antibody bound to all galectin-3 proteins, including *Del*1-118, which consists of the carbohydrate recognition domain only, whereas the monoclonal antibody recognized an epitope located at the N-terminus of galectin-3. The chemically synthesized peptides G3-A9 and G3-C12 similarly bound to all immobilized galectin-3 proteins, including those lacking the entire N-terminal domain and a linker region, but not to control proteins, indicating that these peptides bound to the carbohydrate recognition domain of galectin-3. In contrast, peptide G3-C9 bound all galectin-3 proteins as well as the control protein (Figure 2B), suggesting that binding was non-specific.

Given that the peptides were shown to bind to the carbohydrate recognition domain, the specificity of the three peptides for the carbohydrate recognition domain structure of the galectin-3 protein was further examined. We analyzed peptide binding to plant lectins, including *Vicia villosa* lectin, *Aleuria aurantia* lectin and *Arachis hypogaea* lectin, which specifically recognize *N*-acetylgalactosamine, fucose and TFAg, respectively, as well as to two additional animal galectins, galectin-1 and galectin-4. The galectin family of lectins is defined by a highly conserved carbohydrate recognition domain and affinity for β-galactosides (48). The amino acid sequence identity in the carbohydrate recognition domains among galectins ranges from 20 to 40% (49). Structurally, galectin-1 protein is a prototypic galectin existing as a homodimer comprised of two identical carbohydrate recognition domains (48). Galectin-4 has two distinct carbohydrate recognition domains, one of which is similar to the galectin-3 carbohydrate recognition domain (~35% sequence identity) and a repeating linker region similar to that of galectin-3 (49). Lectins were separated using SDS–PAGE and transferred to nitrocellulose membranes for immunoblotting with anti-galectin-3 peptides. Both the G3-A9 and G3-C12 peptides bound to galectin-3 only and did not recognize galectin-1 or galectin-4 (Figure 2C). To investigate whether peptide binding to galectin-3 was dependent upon the primary peptide sequence, scrambled versions of G3-A9 and G3-C12 were synthesized (G3-A9s and G3-C12s, respectively). The scrambled peptides possessed the same amino acids as the parent peptides but were randomized in their primary sequence. Scrambled peptides such as G3-A9s did not bind to galectin-3 or any of the other lectins examined (data not shown). In contrast to G3-A9 and G3-C12, peptide G3-C9 clearly bound galectin-4 and *Vicia villosa* lectin in addition to galectin-3. However, it was possible that denaturing gel electrophoresis could have preferentially disrupted the structure or carbohydrate-binding functions of some of the lectins

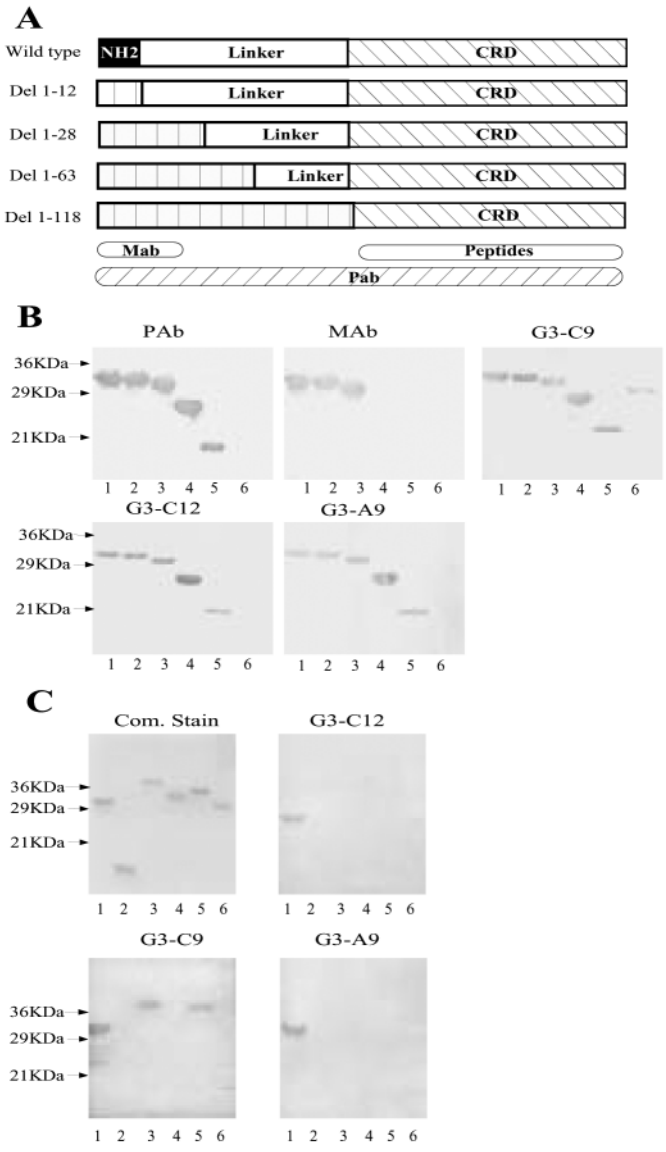

Fig. 2. Mapping the binding site and specificity of peptides for galectin-3. (**A**) Schematic diagram of the primary structure of the truncated galectin-3 proteins and the epitopes that are recognized by anti-galectin-3 antibodies (ovals below the proteins). The truncated proteins are shown in order, from smallest deletion to largest deletion. In each diagram, the vertically hatched areas indicate the deleted structures. (**B**) The binding of peptides to the truncated galectin-3 proteins was analyzed using immunoblot analysis. Purified recombinant galectin-3 (lane 1), truncated galectin-3 proteins (lane 2, *Del*1-12; lane 3, *Del*1-28; lane 4, *Del* 1–63; lane 5, *Del* 1–118) and His_6-tagged DNA-1 monoclonal antibody (61) (lane 6, negative control) were separated by SDS–PAGE and transferred to nitrocellulose membranes. The proteins were detected colorimetrically using biotinylated peptides or galectin-3-specific antibodies (indicated at the top of each panel). Molecular weight markers are labeled to the left. (**C**) Peptide specificity study. Purified recombinant galectin-3 (lane 1), galectin-1 (lane 2), galectin-4 (lane 3), *Aleuria aurantia* lectin (lane 4), *Vicia villosa* lectin (lane 5) and *Arachis hypogaea* lectin (lane 6) were detected colorimetrically using biotinylated peptides and alkaline phosphatase–streptavidin conjugate.

examined. To examine this, lectins were directly spotted onto nitrocellulose and probed with the peptides. As in the gel electrophoresis studies, G3-A9 and G3-C12 bound only to galectin-3. These results, combined with those in Figure 2, suggest that the G3-A9 and G3-C12 peptides specifically interact with the carbohydrate recognition domain of galectin-3 and do not recognize other lectins, even closely related galectins.

Binding of peptides to the surface of cultured carcinoma cells

The galectin-3-binding peptides were selected against purified, immobilized recombinant galectin-3. Thus, we investigated whether the peptides would specifically recognize galectin-3 in its natural conformation present on cultured mammalian cells and whether differential expression of surface galectin-3 would correlate with differential binding by the peptides. As evidenced by staining intensities in laser scanning confocal microscopy studies, peptides G3-A9 and G3-C12 bound most efficiently to J744A cells, expressing the highest levels of galectin-3. There was virtually no binding of these peptides to the galectin-3-negative cell line BT549 (Figure 3A). Heterologous expression of galectin-3 in BT549*trans* cells correlated with peptide binding efficiency. A moderate signal was observed for peptide binding to human breast (MDA-MB-435) and prostate (PC-3 M) carcinoma cells, consistent with the levels of galectin-3 expression in these cell lines. In contrast to G3-A9 and G3-C12, peptide G3-C9 bound uniformly to all cell lines tested, affirming the results of the peptide blotting studies that suggested that this peptide was not specific for galectin-3. The immunocytochemical observations of galectin-3 expression on the various cell lines were confirmed using laser scanning confocal microscopy of intact cells with an anti-galectin-3 monoclonal antibody (Figure 3A) and immunoblotting analyses of cell lysates (data not shown). A similar pattern of monoclonal antibody binding to that of the peptides was observed, suggesting that the degree of peptide binding correlated with the amounts of galectin-3 exposed on the carcinoma cell surfaces.

Binding of TFAg to galectin-3 is inhibited by anti-galectin-3 peptides

We then theorized that the selected galectin-3 carbohydrate recognition domain-binding peptides might act as inhibitors of galectin-3–TFAg interactions. To test this, we first examined the ability of recombinant galectin-3 to interact directly with TFAg in a solid phase binding assay. AlexaFluor 488-labeled ASF bound efficiently to immobilized galectin-3 (Figure 3B). Next, to determine carbohydrate dependence and specificity, competition binding experiments were conducted, using as competing ligands 10 mM *N*-acetyl-lactosamine, 100 μM TFAg-specific *Arachis hypogaea* lectin (50) and 500 mM sucrose. Sucrose, even at concentrations as high as 500 mM, did not inhibit binding of TFAg to galectin-3. Both *Arachis hypogaea* lectin, which binds to and masks the terminal β-galactosides on ASF, and *N*-acetyl-lactosamine, which acts as a soluble competitor for β-galactoside binding, were able to reduce ASF binding to immobilized galectin-3 by ~60%. We then tested whether the two most specific carbohydrate recognition domain-binding peptides, G3-A9 and G3-C12, could inhibit the interaction of galectin-3 with ASF. As revealed by inhibition ELISA, peptides G3-A9 and G3-C12 reduced ASF binding to immobilized galectin-3 in a dose-dependent manner (Figure 3C). Peptides G3-A9 and G3-C12 both exhibited a similar maximal effect at concentrations of 6–12 μM, which is consistent with the calculated binding affinities of these two peptides for galectin-3. Taken together with the data presented in Figure 2, these data suggest that synthetic peptides specific to the galectin-3 carbohydrate

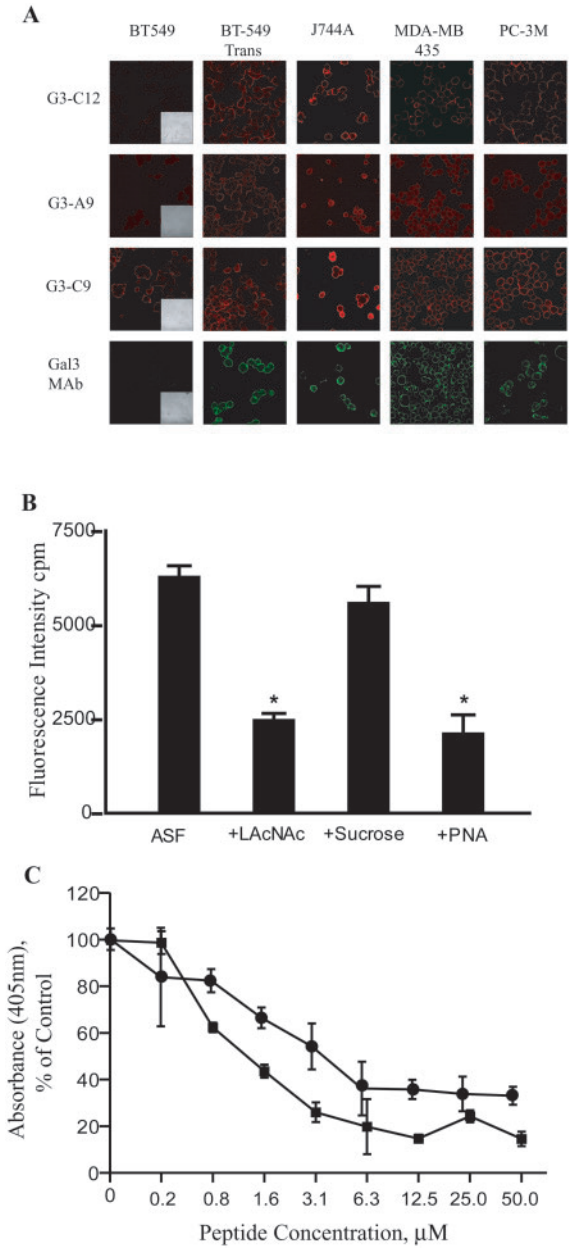

Fig. 3. Galectin-3 peptides bind to carcinoma cells and inhibit binding of galectin-3 to immobilized TFAg. (**A**) Binding of peptides to galectin-3 displayed on cultured human carcinoma cells, including MDA-MB-435 human breast carcinoma cells, PC-3 M human prostate carcinoma cells, BT549 human breast carcinoma cells (negative control) and J744A mouse monocytes (positive control). Binding was detected with NeutrAvidin–Texas Red conjugate (10 μg/ml) or with rat anti-galectin-3 monoclonal antibody followed by AlexaFluor 488-conjugated anti-rat antibody and laser scanning confocal microscopy. (**B** and **C**) Peptides inhibit binding of galectin-3 to TFAg displayed on ASF. (B) Binding of AlexaFluor 488-labeled ASF in solution to immobilized galectin-3 is carbohydrate dependent. Immobilized galectin-3 was incubated with AlexaFluor 488-labeled ASF (in solution) in the presence or absence of 10 mM *N*-acetyl-lactosamine, 500 mM sucrose or 100 mM *Arachis hypogaea* lectin. Binding was detected fluorometrically. All the assays were performed in triplicate and data were analyzed using GraphPad Prism 3.0 software. *Means are significantly different (unpaired *t*-test), $P < 0.0001$. (C) Peptides inhibit binding of galectin-3 (in solution) to TFAg displayed on immobilized ASF in solution. Immobilized ASF was incubated with galectin-3 in solution in the presence of different concentrations of either G3-C12 (1–50 μM) (squares) or G3-A9 (circles). Bound galectin-3 was detected colorimetrically. Wells with no galectin-3 were used as blanks. The assay was performed in triplicate. Percent inhibition was calculated as the decrease in absorbance at 405 nm compared with controls (no peptide).

recognition domain are capable of inhibiting carbohydrate binding to galectin-3.

Inhibition of homotypic adhesion of metastatic human breast carcinoma cells by galectin-3-binding peptides

Metastatic cancer cells homotypically aggregate in a galectin-3-dependent manner to form multicellular intravascular clumps at sites of primary adhesion of tumor cells to the endothelium (3,51). Further, spontaneous carcinoma cell homotypic aggregation is mediated and promoted largely by interaction between cell surface TFAg and galectin-3 molecules (3,21,52). Since our peptides bound cell surface galectin-3 on MDA-MB-435 human breast carcinoma cells and inhibited galectin-3–TFAg interactions, it was of interest to determine whether they would function to inhibit MDA-MB-435 homotypic aggregation. Both G3-A9 and G3-C12, but not a control peptide, inhibited spontaneous MDA-MB-435 human breast carcinoma cell homotypic aggregation in a dose-dependent manner (Figure 4A–C). The maximum reduction (~60%) in homotypic aggregation was observed between 12.5 and 25 μM for G3-C12 (Figure 4A) and 6 and 12.5 μM for G3-A9 (Figure 4B).

Anti-galectin-3 peptides inhibit adhesion of human breast carcinoma cells to the endothelium under flow conditions

The metastatic cascade consists of coordinated sequential steps (3,21,52) in which intravascular heterotypic adhesion between carcinoma cells and the endothelium precedes formation of intravascular carcinoma cell clumps. Heterotypic adhesion functions to slow the forward movement of blood-borne metastatic cells and facilitate their rolling and docking necessary for more stable adhesive interactions to take place (21). Our model of metastasis (21) suggests that galectin-3 expressed on the endothelium may transiently interact with TFAg on the surface of MDA-MB-435 carcinoma cells to slow the forward motion of tumor cells under flow conditions (44). In these studies, we used a bone marrow endothelial line, HBME-1, as a model of endothelium. HBME-1 cells have been extensively used in studies of prostate cell adhesion to bone marrow endothelium (25,53); however, our laboratory has used this cell line extensively to discern the function of galectin-3 in breast cancer adhesion to endothelium. Here, we were interested in examining the effects of the galectin-3-avid peptides G3-A9 and G3-C12 on carcinoma cell adhesion to cultured human bone marrow endothelial cells in a parallel plate laminar flow chamber system, which reconstructs *in vitro* the physical characteristics of *in vivo* microvascular blood flow (4). In our experiments, both rolling and stable adhesion of MDA-MB-435 human breast carcinoma cells on HBME-1 monolayers was significantly inhibited in the presence of anti-galectin-3 peptides, but not of the control peptide (Figure 5A and B; see also Supplementary material). To rule out non-specific effects of peptide addition to the HBME-1 monolayer, in selected experiments anti-galectin-3 and control peptides were added sequentially to the same HBME-1 monolayer. The test peptide (G3-A9 or G3-C12) was infused for ~30 min and inhibition of rolling and stable adhesion was recorded. Tumor cell infusion was halted and the HBME-1 monolayer was perfused with serum-free medium for 20 min. After that, infusion of cancer cells was resumed in the presence of the control peptide. As before, G3-A9 and G3-C12 inhibited MDA-MB-435 carcinoma cell rolling and adhesion. However, once the anti-galectin-3 peptides were washed out of the system and the

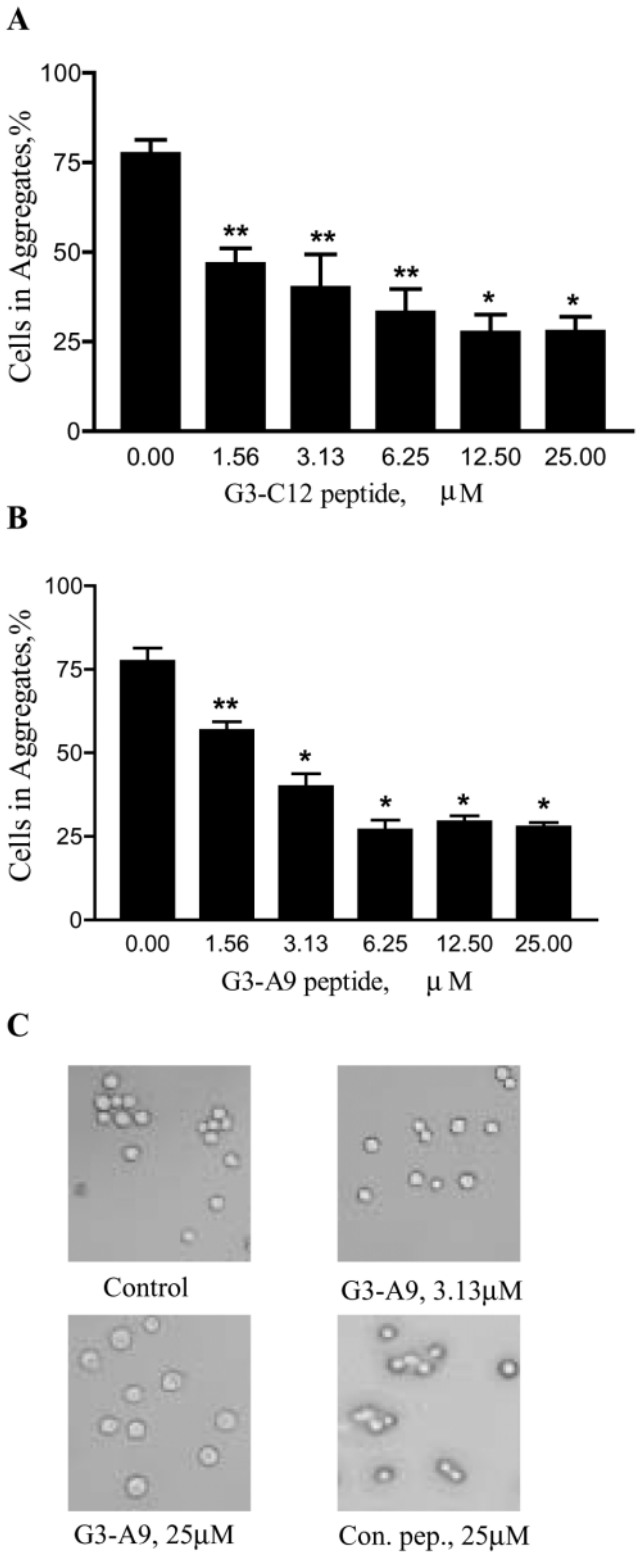

Fig. 4. Galectin-3-binding peptides inhibit homotypic adhesion of MDA-MB-435 human breast carcinoma cells. (**A** and **B**) MDA-MB-435 human breast carcinoma cell suspension was incubated with different concentrations (0–25 μM) of G3-C12, G3-A9 or control peptide. Spontaneous aggregation was detected microscopically by fixing an aliquot of cells on a microscope slide. Four random fields from each slide were examined by transmission microscopy. Cells in aggregates were calculated as percent as described in Materials and methods and plotted. The assay was performed in triplicate. *Means are significantly different (unpaired *t*-test), $P < 0.0001$. **Means are significantly different (unpaired *t*-test), $P < 0.05$. (**C**) Representative transmission photomicrographs.

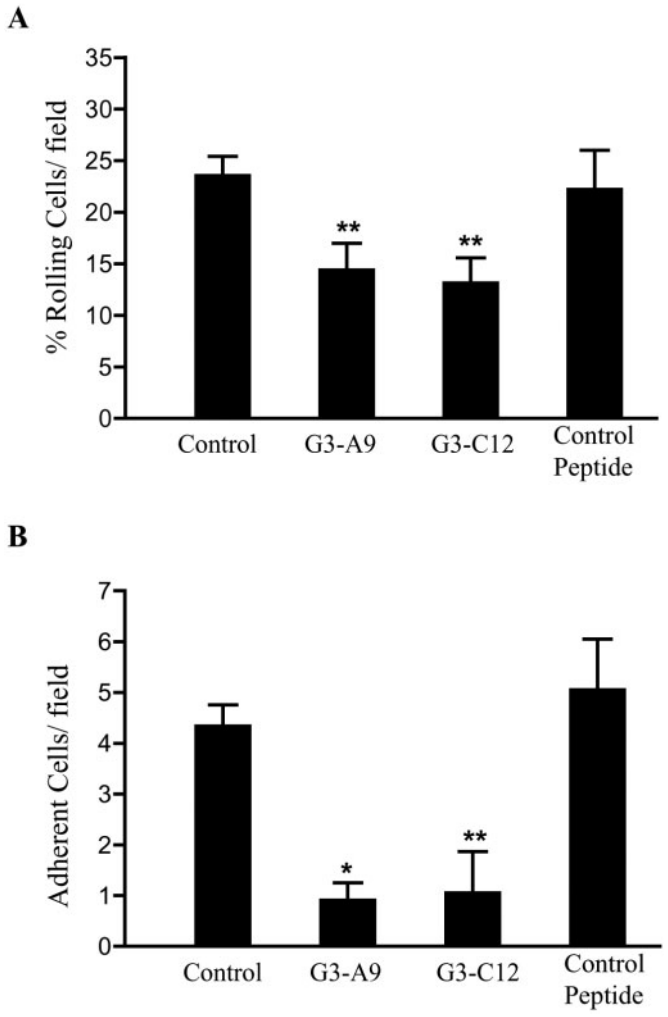

Fig. 5. Galectin-3-binding peptides inhibit rolling and adhesion of MDA-MB-435 human breast carcinoma cells to HBME-1 endothelial cells under flow conditions. (**A**) A single cell suspension of MDA-MB-435 cells was infused across HBME-1 cell monolayers in a laminar flow chamber in the presence or absence of 25 μM G3-A9, G3-C12 or control peptide. (**B**) After stabilization, the number of rolling and adherent tumor cells was recorded. The data are presented as means ± SD of three observation fields from one representative experiment of three independent experiments. *Means are significantly different (unpaired *t*-test), $P < 0.0001$. **Means are significantly different (unpaired *t*-test), $P < 0.05$.

control peptide was introduced instead, the MDA-MB-435 carcinoma cells rolled and adhered (data not shown) as effectively as with fresh untreated or control peptide-treated HBME-1 monolayers (Figure 5A and B). These data demonstrate that under physiologically relevant conditions the anti-galectin-3 peptides inhibit metastasis-related heterotypic adhesion of carcinoma cells to bone marrow endothelium in a manner dependent on transient galectin-3-mediated adhesive interactions.

Discussion

Development of intravascular secondary tumors, the precursors of metastatic lesions (2), requires both heterotypic tumor cell adhesion to endothelium and homotypic adhesion between tumor cells (3,44,51). Previous observations from our laboratory demonstrated that TFAg is able to induce galectin-3

expression and its mobilization to the surface of cultured human endothelial cells *in vitro* (20,51). Furthermore, galectin-3 cell surface translocation occurs intravascularly in well-differentiated microvessels of metastasis-prone tissues in response to metastasis-associated activation by TFAg expressed on circulating glycoproteins and tumor cells (44). Thus, endothelial galectin-3 might function to promote metastatic tumor cell adhesion to blood vessel walls by interacting with TFAg and/or other carbohydrate ligands displayed on tumor cells (21,51). Interactions between tumor cell expressed galectin-3 and TFAg may also contribute to an increased metastatic potential by mediating homotypic adhesion between carcinoma cells (52). This line of homotypic intercellular communication between metastatic cells greatly increases their clonogenic growth and survival (3). Thus, blocking early intravascular galectin-3-mediated tumor cell adhesion has the potential to affect the entire metastatic process and control hematogenous cancer spread. Indeed, efficient inhibition of breast (26,27), colon (26) and prostate (54) cancer metastasis has been achieved using carbohydrate-based galectin-3 inhibitors, modified citrus pectin and lactulosyl-L-leucine (26,27). Further, targeting β-galactoside-mediated interactions using a truncated recombinant galectin-3 carbohydrate recognition domain also resulted in significant inhibition of spontaneous breast cancer metastasis (55).

In this study, we pursued an alternative approach to inhibiting galectin-3 function and β-galactoside-mediated metastasis-associated tumor cell adhesion. We identified short synthetic peptides that bind to the carbohydrate recognition domain of galectin-3 and inhibit the interaction between galectin-3 and its sugar ligand TFAg, thereby interfering with metastasis-associated carcinoma cell heterotypic and homotypic adhesion. Galectin-3-binding peptides were discovered using a combinatorial phage display technology. We identified two peptides (G3-A9 and G3-C12) that bound to purified galectin-3 with high affinity (~80 nM) (Figure 1 and Table I) and recognized cell surface galectin-3 on cultured carcinoma cells and J744A mouse monocyte cells (Figure 2). Studies with full-length and N-terminally truncated galectin-3 proteins indicated that the peptides bound to the carbohydrate recognition domain (Figure 3) and were capable of competing for binding to TFAg displayed on glycoproteins (Figure 4). The peptides may have prevented carbohydrate binding in one of two ways, either by directly occupying the carbohydrate-binding site (carbohydrate mimetic) or by simply occluding access of the carbohydrate to the binding site. In either scenario the peptides interfered with galectin-3 function and, thus, may represent a valuable new approach to inhibiting functionally relevant carbohydrate–lectin interactions. Like carbohydrates, small peptides are capable of modulating carbohydrate recognition domain functions. By blocking the galectin-3–carbohydrate ligand interaction, carbohydrate recognition domain-specific peptides were able to dramatically inhibit both MDA-MB-435 human breast carcinoma cell homotypic and heterotypic adhesion (Figure 5). Similarly, Fukuda and co-workers previously reported that a peptide mimetic of an E-selectin ligand eliminated binding to sialyl Lewis X oligosaccharides and inhibited lung colonization by tumor cells (56). However, their peptide cross-reacted with other selectins, including P-selectin and L-selectin. In our study both G3-A9 and G3-C12 showed remarkable specificity for the galectin-3 carbohydrate recognition domain and did not bind other galectins or plant lectins examined. Although selected from two very different libraries, peptides G3-A9 and G3-C12 shared common amino acids P-(C)-G-P-X-X-X-D-(C)-P that may stabilize an active binding structure. Studies using 'scrambled' peptides indicated that binding was sequence-dependent. Future mutagenesis and structural studies, which are beyond the scope of this paper are being conducted to define the structural basis of the functioning of these peptides.

When both TFAg and galectin-3 are present on carcinoma cells, the interaction between the two is likely involved in metastasis-related homotypic tumor cell adhesion (3,8). Although the role of galectin-3 expressed on carcinoma cells is the subject of much debate (57,58), previous observations from our laboratory have indicated that galectin-3 is clustered at the sites of homotypic contact. The results obtained in the present study suggest that the carbohydrate recognition domain of galectin-3 is exposed and available on the external cell surface, which correlates with other findings that galectin-3 is expressed both on cell surfaces and in the cytoplasm (8). The carbohydrate recognition domain-avid galectin-3 peptides bound to cell surfaces in a manner consistent with the varying levels of galectin-3 cell surface expression known to occur in these cell lines. The ability of the anti-galectin-3 peptides to block the galectin-3 carbohydrate recognition domain was of further functional significance in that the peptides were able to interfere with homotypic carcinoma cell aggregation and adhesion (7,51). Two of the anti-galectin-3 peptides, G3-A9 and G3-C12, reduced carcinoma cell homotypic adhesion by $>50\%$. Taken together, these data suggest that the galectin-3–TFAg interaction is at least partially responsible for homotypic adhesion and that specific blockade of the carbohydrate recognition domain of cell surface galectin-3 is an effective anti-adhesive strategy. However, none of the galectin-3-binding peptides, TFAg-binding peptides or carbohydrate-based compounds which have been examined in this or previous studies (21) were able to inhibit homotypic adhesion completely, suggesting that the galectin-3–TFAg interaction is probably only one of several mechanisms involved in this type of adhesion.

Studies from our laboratory (21) and others (25) suggest that endothelial cell localized galectin-3 may interact with β-galactosides exposed on carcinoma cells to promote adhesion and metastasis. In support of this is the observation that PC-3 human prostate carcinoma cells, which do not express cell surface galectin-3, bind to endothelial cells in a manner that can be inhibited by an anti-galectin-3 monoclonal antibody (25). Similarly, an anti-galectin-3 monoclonal antibody inhibited MDA-MB-435 human breast carcinoma cell rolling and adhesion to human umbilical vein endothelial cell under flow conditions (51). We previously observed that exposure of endothelial cells to TFAg resulted in a 3-fold increase in galectin-3 expression on the endothelial cell surface (3) and that TFAg-binding peptides inhibited heterotypic carcinoma cell adhesion (52). These results imply that the galectin-3–TFAg interaction is involved in this process and that endothelial cell-derived galectin-3 may be able to significantly affect heterotypic carcinoma cell adhesion *in vivo* by creating adhesive 'hot-spots', which may be at least partially responsible for the initial transient carcinoma cell tethering to the endothelium (21,44,51). This event, in turn, may slow the forward movement of carcinoma cells sufficiently to allow other protein–protein interactions to participate in strong and irreversible binding of the carcinoma cells to the vascular endothelium.

We employed the galectin-3 carbohydrate recognition domain-binding peptides as inhibitors of galectin-3–TFAg interactions to analyze the importance of galectin-3 in metastatic cell adhesion to cultured human bone marrow endothelial cells in an assay designed to replicate the *in vivo* environment of the microvasculature. The peptides dramatically inhibited heterotypic adhesion by 60–70% and reduced the percentage of rolling cells in the floating cell population. These findings suggest that galectin-3 is involved in the initial transient contacts, which mature eventually into tight adhesive bonds between cancer cells and endothelium.

Adhesion of carcinoma cells to the endothelium *in vivo* is a complex process involving a variety of mechanisms. Endothelial selectins (59), integrins (60) and other cell surface molecules can promote the adhesion of tumor cells to endothelium in the presence of shear forces that are encountered within the microvascular environment. Recent observations from Al-Mehdi *et al*. demonstrated that endothelium-attached cells are required for the development of secondary tumors, suggesting that early intravascular metastasis formation could be inhibited by intravascular drugs that reduce the attachment of tumor cells to the vascular endothelium (2). Small galectin-3-specific peptides, such as those described here, open new avenues for investigation of galectin-3 functions and the role of carbohydrate–lectin interactions in hematogenous cancer metastasis.

Supplementary material

Supplementary material can be found at: http://www.carcin.oupjournals.org/.

Acknowledgements

The authors thank Drs Avraham Raz and Hakon Leffler for the gifts of galectin-3-expressing vectors, Dr Avraham Raz for providing PC-3M, BT549 and BT549*trans* cells, Dr Janet E.Price for providing MDA-MB-435 cells and Dr Kenneth J.Pienta for providing HBME-1 cells. We would also like to acknowledge the contributions to this work of Marie T.Dickerson, Dr Fabio Gallazi and Dr Olga V.Glinskii for their helpful assistance and Dr George Smith for invaluable advice. This work was supported in part by a Merit Review Award from the Veterans Administration, the Department of Defense DAMD17-03-1-0130 (S.L.D.) and NIH P50 CA103130-01 (Wynn Volkert).

References

1. Chambers,A.F., Groom,A.C. and MacDonald,I.C. (2002) Metastasis: dissemination and growth of cancer cells in metastatic sites. *Nature Rev. Cancer*, **2**, 563–572.
2. Al-Mehdi,A.B., Tozawa,K., Fisher,A.B., Shientag,L., Lee,A. and Muschel,R.J. (2000) Intravascular origin of metastasis from the proliferation of endothelium-attached tumor cells: a new model for metastasis. *Nature Med.*, **6**, 100–102.
3. Glinsky,V.V., Glinsky,G.V., Glinskii,O.V., Huxley,V.H., Turk,J.R., Mossine,V.V., Deutscher,S.L., Pienta,K.J. and Quinn,T.P. (2003) Intravascular metastatic cancer cell homotypic aggregation at the sites of primary attachment to the endothelium. *Cancer Res.*, **63**, 3805–3811.
4. Orr,F.W., Wang,H.H., Lafrenie,R.M., Scherbarth,S. and Nance,D.M. (2000) Interactions between cancer cells and the endothelium in metastasis. *J. Pathol.*, **190**, 310–329.
5. Inohara,H., Akahani,S., Koths,K. and Raz,A. (1996) Interactions between galectin-3 and Mac-2-binding protein mediate cell–cell adhesion. *Cancer Res.*, **56**, 4530–4534.
6. Kannagi,R. (1997) Carbohydrate-mediated cell adhesion involved in hematogenous metastasis of cancer. *Glycoconjugate J.*, **14**, 577–584.
7. Inohara,H. and Raz,A. (1995) Functional evidence that cell surface galectin-3 mediates homotypic cell adhesion. *Cancer Res.*, **55**, 3267–3271.
8. Raz,A. and Lotan,R. (1987) Endogenous galactoside-binding lectins: a new class of functional tumor cell surface molecules related to metastasis. *Cancer Metastasis Rev.*, **6**, 433–452.
9. Le Marer,N. and Hughes,R.C. (1996) Effects of the carbohydrate-binding protein galectin-3 on the invasiveness of human breast carcinoma cells. *J. Cell. Physiol.*, **168**, 51–58.
10. Akahani,S., Nangia-Makker,P., Inohara,H., Kim,H.R. and Raz,A. (1997) Galectin-3: a novel antiapoptotic molecule with a functional BH1 (NWGR) domain of Bcl-2 family. *Cancer Res.*, **57**, 5272–5276.
11. Matarrese,P., Fusco,O., Tinari,N., Natoli,C., Liu,F.T., Semeraro,M.L., Malorni,W. and Iacobelli,S. (2000) Galectin-3 overexpression protects from apoptosis by improving cell adhesion properties. *Int. J. Cancer*, **85**, 545–554.
12. Yu,F., Finley,R.L.,Jr, Raz,A. and Kim,H.R. (2002) Galectin-3 translocates to the perinuclear membranes and inhibits cytochrome c release from the mitochondria. A role for synexin in galectin-3 translocation. *J. Biol. Chem.*, **277**, 15819–15827.
13. Nangia-Makker,P., Honjo,Y., Sarvis,R., Akahani,S., Hogan,V., Pienta,K.J. and Raz,A. (2000) Galectin-3 induces endothelial cell morphogenesis and angiogenesis. *Am. J. Pathol.*, **156**, 899–909.
14. Gillenwater,A., Xu,X.C., el-Naggar,A.K., Clayman,G.L. and Lotan,R. (1996) Expression of galectins in head and neck squamous cell carcinoma. *Head Neck*, **18**, 422–432.
15. Raz,A. and Lotan,R. (1981) Lectin-like activities associated with human and murine neoplastic cells. *Cancer Res.*, **41**, 3642–3647.
16. Raz,A., Zhu,D.G., Hogan,V., Shah,N., Raz,T., Karkash,R., Pazerini,G. and Carmi,P. (1990) Evidence for the role of 34-kDa galactoside-binding lectin in transformation and metastasis. *Int. J. Cancer*, **46**, 871–877.
17. Ochieng,J., Warfield,P., Green-Jarvis,B. and Fentie,I. (1999) Galectin-3 regulates the adhesive interaction between breast carcinoma cells and elastin. *J. Cell. Biochem.*, **75**, 505–514.
18. Meromsky,L., Lotan,R. and Raz,A. (1986) Implications of endogenous tumor cell surface lectins as mediators of cellular interactions and lung colonization. *Cancer Res.*, **46**, 5270–5275.
19. Springer,G.F. (1984) T and Tn, general carcinoma autoantigens. *Science*, **224**, 1198–1206.
20. Baldus,S.E., Hanisch,F.G., Monaca,E., Karsten,U.R., Zirbes,T.K., Thiele,J. and Dienes,H.P. (1999) Immunoreactivity of Thomsen-Friedenreich (TF) antigen in human neoplasms: the importance of carrier-specific glycotope expression on MUC1. *Histol. Histopathol.*, **14**, 1153–1158.
21. Glinsky,V.V., Glinsky,G.V., Rittenhouse-Olson,K., Huflejt,M.E., Glinskii,O.V., Deutscher,S.L. and Quinn,T.P. (2001) The role of Thomsen-Friedenreich antigen in adhesion of human breast and prostate cancer cells to the endothelium. *Cancer Res.*, **61**, 4851–4857.
22. Chung,Y.S., Yamashita,Y., Kato,Y., Nakata,B., Sawada,T. and Sowa,M. (1996) Prognostic significance of T antigen expression in patients with gastric carcinoma. *Cancer*, **77**, 1768–1773.
23. Baldus,S.E., Hanisch,F.G., Kotlarek,G.M., Zirbes,T.K., Thiele,J., Isenberg,J., Karsten,U.R., Devine,P.L. and Dienes,H.P. (1998) Coexpression of MUC1 mucin peptide core and the Thomsen-Friedenreich antigen in colorectal neoplasms. *Cancer*, **82**, 1019–1027.
24. Springer,G.F. (1989) Tn epitope (N-acetyl-D-galactosamine alpha-O-serine/threonine) density in primary breast carcinoma: a functional predictor of aggressiveness. *Mol. Immunol.*, **26**, 1–5.
25. Lehr,J.E. and Pienta,K.J. (1998) Preferential adhesion of prostate cancer cells to a human bone marrow endothelial cell line. *J. Natl Cancer Inst.*, **90**, 118–123.
26. Nangia-Makker,P., Hogan,V., Honjo,Y., Baccarini,S., Tait,L., Bresalier,R. and Raz,A. (2002) Inhibition of human cancer cell growth and metastasis in nude mice by oral intake of modified citrus pectin. *J. Natl Cancer Inst.*, **94**, 1854–1862.
27. Glinsky,G.V., Price,J.E., Glinsky,V.V., Mossine,V.V., Kiriakova,G. and Metcalf,J.B. (1996) Inhibition of human breast cancer metastasis in nude mice by synthetic glycoamines. *Cancer Res.*, **56**, 5319–5324.
28. Bachhawat-Sikder,K., Thomas,C.J. and Surolia,A. (2001) Thermodynamic analysis of the binding of galactose and poly-N-acetyllactosamine derivatives to human galectin-3. *FEBS Lett.*, **500**, 75–79.
29. Mehta,P., Cummings,R.D. and McEver,R.P. (1998) Affinity and kinetic analysis of P-selectin binding to P-selectin glycoprotein ligand-1. *J. Biol. Chem.*, **273**, 32506–32513.
30. Nicholson,M.W., Barclay,A.N., Singer,M.S., Rosen,S.D. and van der Merwe,P.A. (1998) Affinity and kinetic analysis of L-selectin (CD62L) binding to glycosylation-dependent cell-adhesion molecule-1. *J. Biol. Chem.*, **273**, 763–770.
31. Landon,L.A. and Deutscher,S.L. (2003) Combinatorial discovery of tumor targeting peptides using phage display. *J. Cell. Biochem.*, **90**, 509–517.

32. Landon,L.A., Zou,J. and Deutscher,S.L. (2004) Is phage display on target for developing peptide-based cancer drugs? *Curr. Drug Discov. Technol.*, **1**, 113–132.
33. Landon,L.A., Peletskaya,E.N., Glinsky,V.V., Karasseva,N., Quinn,T.P. and Deutscher,S.L. (2003) Combinatorial evolution of high affinity peptides that bind to the Thomsen-Friedenreich carcinoma antigen. *J. Protein Chem.*, **22**, 193–204.
34. Landon,L.A., Zou,J. and Deutscher,S.L. (2003) An effective combinatorial strategy to increase affinity of carbohydrate binding by peptides. *Mol. Divers.*, **8**, 35–50.
35. Ochieng,J., Platt,D., Tait,L., Hogan,V., Raz,T., Carmi,P. and Raz,A. (1993) Structure–function relationship of a recombinant human galactoside-binding protein. *Biochemistry*, **32**, 4455–4460.
36. Smith,G.P. and Scott,J.K. (1993) Libraries of peptides and proteins displayed on filamentous phage. *Methods Enzymol.*, **217**, 228–257.
37. Peletskaya,E.N., Glinsky,G., Deutscher,S.L. and Quinn,T.P. (1996) Identification of peptide sequences that bind the Thomsen-Friedenreich cancer-associated glycoantigen from bacteriophage peptide display libraries. *Mol. Divers.*, **2**, 13–18.
38. Haas,S.J. and Smith,G.P. (1993) Rapid sequencing of viral DNA from filamentous bacteriophage. *Biotechniques*, **15**, 422–424, 426–428, 431.
39. Peletskaya,E.N., Glinsky,V.V., Glinsky,G.V., Deutscher,S.L. and Quinn,T.P. (1997) Characterization of peptides that bind the tumor-associated Thomsen-Friedenreich antigen selected from bacteriophage display libraries. *J. Mol. Biol.*, **270**, 374–384.
40. Laemmli,U.K. (1970) Cleavage of structural proteins during the assembly of the head of bacteriophage T4. *Nature*, **227**, 680–685.
41. Landon,L.A., Harden,W., Illy,C. and Deutscher,S.L. (2004) High throughput fluorescence spectroscopic analysis of binding affinity of peptides displayed on bacteriophage. *Anal. Biochem.*, **331**, 60–67.
42. Kim,C., Paulus,B.F. and Wold,M.S. (1994) Interactions of human replication protein A with oligonucleotides. *Biochemistry*, **33**, 14197–14206.
43. Andre,S., Kojima,S., Yamazaki,N., Fink,C., Kaltner,H., Kayser,K. and Gabius,H.J. (1999) Galectins-1 and -3 and their ligands in tumor biology. Non-uniform properties in cell-surface presentation and modulation of adhesion to matrix glycoproteins for various tumor cell lines, in biodistribution of free and liposome-bound galectins and in their expression by breast and colorectal carcinomas with/without metastatic propensity. *J. Cancer Res. Clin. Oncol.*, **125**, 461–474.
44. Glinskii,O.V., Turk,J.R., Pienta,K.J., Huxley,V.H. and Glinsky,V.V. (2004) Evidence of porcine and human endothelium activation by cancer-associated carbohydrates expressed on glycoproteins and tumour cells. *J. Physiol. (Lond.)*, **554**, 89–99.
45. Edge,A.S. and Spiro,R.G. (1987) Presence of an O-glycosidically linked hexasaccharide in fetuin. *J. Biol. Chem.*, **262**, 16135–16141.
46. Green,E.D., Adelt,G., Baenziger,J.U., Wilson,S. and Van Halbeek,H. (1988) The asparagine-linked oligosaccharides on bovine fetuin. Structural analysis of N-glycanase-released oligosaccharides by 500-megahertz 1H NMR spectroscopy. *J. Biol. Chem.*, **263**, 18253–18268.
47. Cumming,D.A., Hellerqvist,C.G., Harris-Brandts,M., Michnick,S.W., Carver,J.P. and Bendiak,B. (1989) Structures of asparagine-linked oligosaccharides of the glycoprotein fetuin having sialic acid linked to N-acetylglucosamine. *Biochemistry*, **28**, 6500–6512.
48. Barondes,S.H., Cooper,D.N., Gitt,M.A. and Leffler,H. (1994) Galectins. Structure and function of a large family of animal lectins. *J. Biol. Chem.*, **269**, 20807–20810.
49. Oda,Y., Herrmann,J., Gitt,M.A., Turck,C.W., Burlingame,A.L., Barondes,S.H. and Leffler,H. (1993) Soluble lactose-binding lectin from rat intestine with two different carbohydrate-binding domains in the same peptide chain. *J. Biol. Chem.*, **268**, 5929–5939.
50. Pereira,M.E., Kabat,E.A., Lotan,R. and Sharon,N. (1976) Immunochemical studies on the specificity of the peanut (*Arachis hypogaea*) agglutinin. *Carbohydr. Res.*, **51**, 107–118.
51. Khaldoyanidi,S.K., Glinsky,V.V., Sikora,L., Glinskii,A.B., Mossine,V.V., Quinn,T.P., Glinsky,G.V. and Sriramarao,P. (2003) MDA-MB-435 human breast carcinoma cell homo- and heterotypic adhesion under flow conditions is mediated in part by Thomsen-Friedenreich antigen-galectin-3 interactions. *J. Biol. Chem.*, **278**, 4127–4134.
52. Glinsky,V.V., Huflejt,M.E., Glinsky,G.V., Deutscher,S.L. and Quinn,T.P. (2000) Effects of Thomsen-Friedenreich antigen-specific peptide P-30 on beta-galactoside-mediated homotypic aggregation and adhesion to the endothelium of MDA-MB-435 human breast carcinoma cells. *Cancer Res.*, **60**, 2584–2588.
53. Cooper,C.R., McLean,L., Walsh,M., Taylor,J., Hayasaka,S., Bhatia,J. and Pienta,K.J. (2000) Preferential adhesion of prostate cancer cells to bone is mediated by binding to bone marrow endothelial cells as compared to extracellular matrix components *in vitro*. *Clin. Cancer Res.*, **6**, 4839–4847.
54. Pienta,K.J., Naik,H., Akhtar,A., Yamazaki,K., Replogle,T.S., Lehr,J., Donat,T.L., Tait,L., Hogan,V. and Raz,A. (1995) Inhibition of spontaneous metastasis in a rat prostate cancer model by oral administration of modified citrus pectin. *J. Natl Cancer Inst.*, **87**, 348–353.
55. John,C.M., Leffler,H., Kahl-Knutsson,B., Svensson,I. and Jarvis,G.A. (2003) Truncated galectin-3 inhibits tumor growth and metastasis in orthotopic nude mouse model of human breast cancer. *Clin. Cancer Res.*, **9**, 2374–2383.
56. Fukuda,M.N., Ohyama,C., Lowitz,K., Matsuo,O., Pasqualini,R., Ruoslahti,E. and Fukuda,M. (2000) A peptide mimic of E-selectin ligand inhibits sialyl Lewis X-dependent lung colonization of tumor cells. *Cancer Res.*, **60**, 450–456.
57. Lotz,M.M., Andrews,C.W.,Jr, Korzelius,C.A., Lee,E.C., Steele,G.D.,Jr, Clarke,A. and Mercurio,A.M. (1993) Decreased expression of Mac-2 (carbohydrate binding protein 35) and loss of its nuclear localization are associated with the neoplastic progression of colon carcinoma. *Proc. Natl Acad. Sci. USA*, **90**, 3466–3470.
58. Schoeppner,H.L., Raz,A., Ho,S.B. and Bresalier,R.S. (1995) Expression of an endogenous galactose-binding lectin correlates with neoplastic progression in the colon. *Cancer*, **75**, 2818–2826.
59. Tozeren,A., Kleinman,H.K., Grant,D.S., Morales,D., Mercurio,A.M. and Byers,S.W. (1995) E-selectin-mediated dynamic interactions of breast- and colon-cancer cells with endothelial-cell monolayers. *Int. J. Cancer*, **60**, 426–431.
60. Lafrenie,R.M., Gallo,S., Podor,T.J., Buchanan,M.R. and Orr,F.W. (1994) The relative roles of vitronectin receptor, E-selectin and alpha 4 beta 1 in cancer cell adhesion to interleukin-1-treated endothelial cells. *Eur. J. Cancer*, **30A**, 2151–2158.
61. Komissarov,A.A., Calcutt,M.J., Marchbank,M.T., Peletskaya,E.N. and Deutsher,S.L. (1996) Equilibrium binding studies of recombinant anti-single-stranded DNA Fab. Role of heavy chain complementarity-determining regions. *J. Biol. Chem.*, **271**, 12241–12246.

Received August 24, 2004; revised October 7, 2004; accepted October 26, 2004